Research Article

Formulation and In Vitro-In Vivo Evaluation of ICARIIN-Curcumin Nano-Transfersome-Loaded Rapid-Dissolving Microneedles for Osteoporosis Management

Richa Singh[1], Dr. Sushila kaura[2]

[1]Research Scholar, Jayoti Vidyapeeth Women's University, Jaipur, Rajasthan, India
[2]Professor, Jayoti Vidyapeeth Women's University, Jaipur, Rajasthan, India

Corresponding author:
Richa Singh
Email Id: richasingh13may@gmail.com

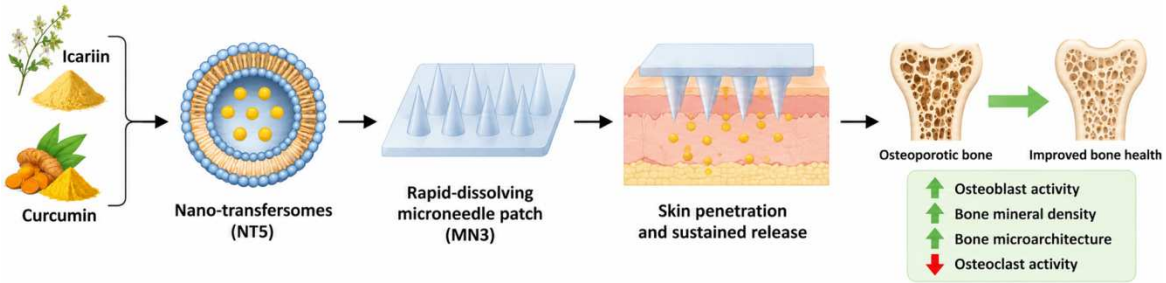
ABSTRACT

Osteoporosis is characterized by reduced bone mass and deterioration of bone microarchitecture due to an imbalance between bone formation and resorption. Icariin and curcumin possess osteoprotective potential, but their poor solubility limits their delivery. This study aimed to develop an icariin-curcumin co-loaded nano-transfersome-based rapid-dissolving microneedle (RDMN) patch for osteoporosis management. Nano-transfersomes were prepared by thin-film hydration and optimized based on vesicle size, PDI, zeta potential and entrapment efficiency. The optimized formulation was incorporated into PVA-PVP microneedles and evaluated for physicochemical properties, drug release, in-vitro osteoprotective activity and in-vivo efficacy in an ovariectomized rat model. NT5 showed a vesicle size of 126.4 ± 3.9 nm, PDI of 0.158 ± 0.010, and high entrapment efficiencies for icariin (93.24 ± 1.08%) and curcumin (95.18 ± 1.02%). The optimized MN3 exhibited satisfactory mechanical strength, 92.8 ± 2.4% insertion efficiency and rapid dissolution. MN3 sustained drug release for 24 h and enhanced osteoblast proliferation, ALP activity and mineralization while reducing TRAP activity and osteoclast-related marker expression. In ovariectomized rats, MN3 improved biochemical parameters, increased bone mineral density to 0.207 ± 0.009 g/cm², and improved bone microarchitecture compared with the osteoporotic control. Thus, the icariin-curcumin nano-transfersome-loaded RDMN patch demonstrated promising osteoprotective activity and represents a potential advanced delivery approach for osteoporosis.

Keywords: Icariin; Curcumin; Nano-transfersomes; Rapid-dissolving microneedles; Osteoporosis; Osteoblasts; Osteoclasts; Bone mineral density.

How to cite this article: Singh R, Kaura S., Formulation and In Vitro-In Vivo Evaluation of Icariin-Curcumin Nano-Transfersome-Loaded Rapid-Dissolving Microneedles for Osteoporosis Management. Int J Drug Deliv Technol. 2026;16(89s): 232-245; DOI: 10.25258/ijddt.16.89s.23

Graphical Abstract:



1. INTRODUCTION

Osteoporosis is a chronic metabolic skeletal disorder characterized by deterioration of bone mass and microarchitecture, resulting in reduced bone strength and an increased risk of fragility fractures. The disease develops when the physiological balance between bone formation and bone resorption is disturbed, with excessive osteoclastic bone resorption exceeding osteoblastic bone formation. Osteoblasts, osteoclasts, and osteocytes participate in a highly regulated remodeling process that maintains skeletal homeostasis; disruption of this process due to aging, estrogen deficiency, oxidative stress, inflammation, metabolic abnormalities, and other risk factors can progressively compromise bone quality and strength (Compston et al., 2019; Fu et al., 2025). The increasing prevalence of

osteoporosis with population aging has consequently stimulated the investigation of therapeutic approaches that can simultaneously regulate bone formation, bone resorption, inflammation, and oxidative stress.

Conventional pharmacological management of osteoporosis includes antiresorptive and anabolic therapies designed to reduce bone loss or stimulate bone formation. Although these treatments have substantially improved osteoporosis management, limitations related to long-term administration, adverse effects, patient adherence, and route of administration continue to encourage the development of alternative therapeutic strategies and advanced drug-delivery systems. Consequently, naturally derived bioactive compounds with multiple pharmacological activities have attracted increasing attention as potential candidates for the management of skeletal disorders.

Among these compounds, icariin (ICA), a prenylated flavonoid glycoside predominantly obtained from *Epimedium* species, has emerged as one of the extensively investigated phytoconstituents for osteoporosis. Icariin has demonstrated osteogenic, anti-osteoclastogenic, anti-inflammatory, and antioxidant properties in experimental studies. Fu et al. (2025) systematically reviewed 182 publications and reported that icariin improved bone mineral density and bone microarchitecture across several experimental osteoporosis models, including postmenopausal, glucocorticoid-induced, aging, and diabetic osteoporosis. The review further demonstrated that icariin may exert a dual regulatory effect by promoting osteogenesis while suppressing osteoclastogenesis and may influence multiple biological processes, including oxidative stress, inflammation, autophagy, and iron metabolism (Fu et al., 2025).

Recent experimental evidence has further elucidated the molecular basis of icariin-mediated osteogenesis. Zhao et al. (2025) demonstrated that icariin promoted osteogenic differentiation and mineralization of bone marrow mesenchymal stem cells and attenuated bone loss in ovariectomized rats. The study associated these effects with modulation of the Hippo/TAZ signaling pathway, with icariin reducing MST1 and TAZ phosphorylation and consequently enhancing TAZ-mediated osteogenic signaling. In the ovariectomized rat model, icariin improved bone mineral density and trabecular microarchitecture and increased the expression of osteogenic markers including alkaline phosphatase, Runx2, and osteocalcin (Zhao et al., 2025).

Despite its promising pharmacological properties, icariin presents important pharmaceutical challenges. Its physicochemical characteristics can restrict aqueous solubility, dissolution, permeability, and systemic exposure, thereby limiting the therapeutic performance of conventional formulations. Accordingly, considerable research has focused on improving the delivery of icariin through pharmaceutical technologies and nanocarrier systems. The recent systematic review by Fu et al. (2025) specifically emphasized that innovative drug-delivery systems and advanced biomaterials can improve the targeting and therapeutic performance of icariin, highlighting formulation development as an important component of future icariin-based osteoporosis therapy.

Curcumin (CUR), the principal polyphenolic constituent of *Curcuma longa*, represents another promising natural bioactive compound for osteoporosis research. Curcumin possesses antioxidant and anti-inflammatory activities and has been investigated for its ability to modulate osteoblast and osteoclast functions. Its effects on bone remodeling have been associated with multiple molecular pathways, including OPG/RANKL, NF-κB, Wnt/β-catenin, MAPK, and TGF-β/Smad signaling. A 2025 systematic review and meta-analysis by Yang et al. involving 17 preclinical studies and 282 animals reported that curcumin significantly increased femoral and tibial bone mineral density and improved trabecular parameters including bone volume fraction, trabecular number, trabecular thickness, and trabecular separation. The analysis also reported reductions in bone-resorption markers such as CTX-1 and TRAP-5b and increases in osteogenic markers including osteocalcin and alkaline phosphatase (Yang et al., 2025).

More recent evidence continues to support the potential of curcumin in experimental osteoporosis. A 2026 preclinical meta-analysis incorporating 23 controlled in vivo studies reported significant improvements in femoral bone mineral density, trabecular microarchitecture, and biomechanical strength following curcumin administration. The study also identified effects on bone-remodeling and oxidative-stress-related markers (2026). However, the authors emphasized that exploratory dose-response observations should not be interpreted as validated optimal clinical doses because the analysis was based on a limited number of study-level observations.

The pharmaceutical application of curcumin, however, is limited by its poor aqueous solubility, physicochemical instability, limited absorption, extensive metabolism, and low systemic bioavailability. These properties have encouraged the development of advanced delivery approaches capable of improving curcumin solubilization, stability, absorption, and therapeutic performance. Yadav (2026) reviewed the pharmacological activities and pharmaceutical limitations of curcumin and identified enhanced delivery systems as an important direction for improving its therapeutic utilization.

The therapeutic rationale for combining icariin and curcumin arises from their complementary biological activities. Icariin has demonstrated prominent effects on osteogenic differentiation and osteoclast regulation, whereas curcumin provides additional antioxidant and anti-inflammatory effects and can influence several signaling pathways involved in bone remodeling (Fu et al., 2025; Yang et al., 2025). Therefore, simultaneous delivery of these phytoconstituents may provide a multi-target approach to osteoporosis by addressing different biological components of skeletal deterioration. However, the physicochemical limitations of both compounds make the development of a suitable delivery platform particularly important.

The application of nanotechnology in phytomedicine has provided new opportunities for addressing the limitations of naturally derived bioactive compounds. Nanocarriers can improve the apparent solubility, stability, protection, cellular interaction, and delivery of poorly soluble phytoconstituents. Wasiullah et al. (2025), in a systematic review published in the *Global Journal of Pharmaceutical and Scientific Research*, highlighted the increasing application of nanotechnology in phytomedicine and drug development and discussed the potential of nanoscale delivery systems to overcome formulation and bioavailability limitations associated with plant-derived therapeutic compounds.

Among different nanocarrier platforms, nano-transfersomes are particularly attractive for transdermal drug delivery because of their highly deformable lipid membranes. Transfersomes are generally composed of phospholipids and edge activators, which impart flexibility and elasticity to the vesicular membrane. This deformability allows the vesicles to interact with and potentially traverse the highly organized lipid structure of the stratum corneum, thereby enhancing the delivery of incorporated molecules across the skin. The application of deformable vesicular systems has therefore received considerable attention for improving the transdermal delivery of compounds with unfavorable physicochemical characteristics.

Nevertheless, the stratum corneum remains the principal physiological barrier to efficient transdermal drug delivery. Its highly organized lipid-protein structure restricts the penetration of many therapeutic molecules, particularly compounds that do not possess favorable molecular size, lipophilicity, and partitioning characteristics. Conventional topical and transdermal systems may therefore exhibit limited delivery efficiency when applied to poorly permeable compounds. This limitation has encouraged the development of physical and technological strategies capable of temporarily bypassing the stratum corneum.

Microneedle technology has emerged as one such strategy. Microneedles consist of micron-scale projections capable of penetrating the stratum corneum and creating transient pathways through which therapeutic agents can be delivered. Compared with conventional hypodermic injections, microneedles can provide minimally invasive administration while potentially improving patient acceptability. They can also overcome some of the limitations associated with passive transdermal delivery by providing direct access beyond the principal skin barrier.

Among the different microneedle platforms, rapid-dissolving microneedles (RDMNs) have received increasing attention because they can be fabricated using water-soluble or biodegradable polymers that dissolve after insertion into the skin. Following insertion, the polymeric matrix hydrates and dissolves, releasing the incorporated therapeutic payload without generating persistent sharp waste. Zhuo et al. (2025) highlighted the ability of dissolving microneedles to combine the advantages of transdermal delivery and minimally invasive administration while providing opportunities for the delivery of both small and larger therapeutic molecules.

Despite their considerable potential, the translation of dissolving microneedles into pharmaceutical products remains challenging. Important formulation and manufacturing considerations include mechanical strength, insertion capability, drug-loading capacity, dissolution behavior, dose uniformity, polymer selection, stability, scalability, and quality control. Moawad et al. (2025) emphasized that although microneedles represent a promising minimally invasive delivery technology, their translation into clinical applications remains limited by formulation, manufacturing, regulatory, and reproducibility challenges. These considerations are particularly important when a complex nanocarrier such as nano-transfersomes is incorporated into a dissolving microneedle matrix.

The integration of nano-transfersomes with rapid-dissolving microneedles therefore represents a potentially useful strategy for improving transdermal delivery. In such a system, nano-transfersomes can encapsulate and protect poorly soluble phytoconstituents, while the microneedle array can temporarily bypass the stratum corneum and facilitate deposition of the nanovesicles within the skin. The combination may consequently address two major formulation barriers simultaneously: the poor aqueous/biopharmaceutical properties of the active compounds and the barrier

function of the stratum corneum. Recent research on integrated nanotransfersome-microneedle systems further supports the feasibility of this approach for improving transdermal drug delivery and pharmacokinetic performance.

The development of such advanced systems is consistent with the broader direction of pharmaceutical nanotechnology. Firoz and Parmar (2026) developed lurasidone-loaded niosomes and demonstrated that the optimized formulation exhibited nanoscale vesicle characteristics, high entrapment efficiency, sustained drug release, and improved formulation stability, illustrating the continuing relevance of nanovesicular approaches in contemporary pharmaceutical research.

Although substantial evidence exists regarding the individual anti-osteoporotic potential of icariin and curcumin and the application of nanotechnology for improving phytoconstituent delivery, the development of an icariin-curcumin co-loaded nano-transfersomal system integrated into a rapid-dissolving microneedle patch for osteoporosis represents a comparatively unexplored formulation strategy. Recent research has established the potential of icariin to regulate osteogenic and osteoclastogenic pathways and has demonstrated the ability of advanced delivery systems to improve its therapeutic performance (Fu et al., 2025; Zhao et al., 2025). Similarly, preclinical evidence supports the anti-osteoporotic effects of curcumin, although its poor bioavailability continues to represent a significant pharmaceutical challenge (Yang et al., 2025). Meanwhile, contemporary research on nanotechnology and vesicular drug delivery provides a rational technological foundation for improving the delivery of these phytoconstituents (Wasiullah et al., 2025; Yadav, 2026; Kumar et al., 2026).

Therefore, the present study was designed to develop and evaluate a rapid-dissolving microneedle patch loaded with icariin-curcumin nano-transfersomes for osteoporosis therapy. The study involves the formulation and optimization of icariin-curcumin nano-transfersomes, their incorporation into a rapidly dissolving microneedle matrix, and comprehensive evaluation of the resulting system with respect to particle size, polydispersity index, zeta potential, morphology, drug content, encapsulation efficiency, mechanical strength, insertion ability, dissolution behavior, in vitro drug release, ex vivo skin permeation, and in vivo therapeutic performance. The proposed system is intended to combine the complementary pharmacological activities of icariin and curcumin with the nanocarrier properties of nano-transfersomes and the barrier-bypassing capability of rapid-dissolving microneedles. This integrated approach may provide a novel pharmaceutical platform for improving the delivery of poorly soluble phytoconstituents and investigating their potential in osteoporosis management.

2. MATERIALS AND METHODS

2.1 Materials

Icariin and curcumin were selected as the active phytoconstituents for the development of the anti-osteoporotic delivery system. Phospholipid and Tween 80 were used for preparation of nano-transfersomes, while polyvinyl alcohol (PVA) and polyvinylpyrrolidone (PVP) were used for fabrication of the rapid-dissolving microneedle (RDMN) patch. All other solvents, reagents, and analytical-grade chemicals were obtained from standard commercial sources and used as received.

2.2 Preformulation Studies

The selected phytoconstituents were subjected to preliminary preformulation studies, including organoleptic characteristics, solubility, melting point determination, UV-visible spectrophotometric analysis, and determination of the maximum absorption wavelength (λmax). Calibration curves of icariin and curcumin were prepared using appropriate concentrations and analytical conditions. Solubility studies were performed in triplicate.

2.3 Drug-Excipient Compatibility Study

Compatibility between icariin, curcumin, and the selected excipients was investigated using Fourier-transform infrared spectroscopy (FTIR). Spectra of the individual drugs, excipients, and their physical mixtures were recorded and compared for characteristic functional-group peaks and possible chemical interactions.

2.4 Preparation of Icariin-Curcumin Nano-Transfersomes

Icariin-curcumin nano-transfersomes were prepared by the thin-film hydration method using phospholipid as the vesicular-forming lipid and Tween 80 as the edge activator. Icariin and curcumin were maintained at 10 mg each per formulation. Phospholipid concentration was varied from 50-150 mg and Tween 80 from 10-30 mg, while the aqueous phase was adjusted to 10 mL. Nine formulations (NT1-NT9) were prepared by varying the phospholipid and Tween 80 concentrations. The lipid and drugs were dissolved in a suitable volatile organic solvent system and subjected to rotary evaporation under reduced pressure to form a thin lipid film. The film was further dried under vacuum and

hydrated with the aqueous phase containing the required amount of Tween 80. The resulting dispersion was sonicated and allowed to equilibrate before characterization.

2.5 Optimization and Characterization of Nano-Transfersomes

The nano-transfersomes were optimized based on vesicle size, polydispersity index (PDI), zeta potential, and entrapment efficiency (EE) of icariin and curcumin. Vesicle size and PDI were determined by dynamic light scattering, while zeta potential was measured by electrophoretic light scattering. Morphology was examined by transmission electron microscopy (TEM). For determination of EE, the formulation was separated from unentrapped drug by centrifugation. The amount of free drug was quantified and EE was calculated as:

$$\textbf{EE (\%)} = [(\text{Total drug} - \text{Free drug}) / \text{Total drug}] \times 100$$

Drug loading was calculated from the amount of entrapped drug relative to the total weight of the nano-transfersomes. Vesicle deformability was evaluated by extrusion through a suitable membrane to assess the ability of the vesicles to deform under mechanical stress.

2.6 Development of Rapid-Dissolving Microneedle Patch

PVA and PVP were selected as matrix-forming polymers for the RDMN patch. PVA provided mechanical strength, whereas PVP facilitated rapid hydration and dissolution. The polymers were maintained at a 1:2 PVA ratio. Five polymeric formulations (MN1-MN5) containing total polymer concentrations of 10, 15, 20, 25, and 30% w/v, respectively, were prepared. PVA and PVP were dissolved separately and subsequently combined. The polymeric solution was deaerated before incorporation of the optimized icariin-curcumin nano-transfersome dispersion under gentle stirring.

2.7 Fabrication and Evaluation of RDMN Patches

The polymeric nano-transfersome formulation was cast into a polydimethylsiloxane (PDMS) microneedle mold. The mold was centrifuged at 4000 rpm for 30 min to facilitate filling of the microneedle cavities. Excess formulation was removed, and a backing layer was applied where required. The molds were dried at approximately 40°C until solidification, followed by careful demolding.The prepared patches were evaluated for physical appearance, needle morphology, dimensions, mechanical strength, skin insertion ability, dissolution behavior, drug content, and moisture content. Microneedle morphology and dimensions were examined using optical microscopy and/or scanning electron microscopy. Mechanical strength was assessed using a suitable texture-analysis procedure, while insertion efficiency was evaluated using ex vivo skin. Dissolution time was determined in an aqueous or simulated physiological medium. Drug content was determined after dissolving an accurately weighed portion of the patch in a suitable solvent, followed by quantitative analysis of icariin and curcumin. Moisture content was determined gravimetrically.

2.8 In Vitro Drug Release Study

In vitro release of icariin and curcumin from the optimized nano-transfersome-loaded RDMN patch was investigated using a diffusion-based method under controlled temperature and agitation conditions. Samples were withdrawn at predetermined time intervals and replaced with an equal volume of fresh release medium. The concentrations of icariin and curcumin were determined using the respective analytical methods, and cumulative drug release was calculated.

2.9 Ex Vivo Skin Permeation Study

Ex vivo permeation was evaluated using a Franz diffusion cell containing excised skin. The skin was positioned between the donor and receptor compartments with the stratum corneum facing the donor compartment. The receptor medium was maintained at controlled temperature with continuous stirring. Samples were withdrawn at predetermined intervals and analyzed for icariin and curcumin. Following the experiment, the skin was extracted to determine the amount of drug retained within the tissue. The steady-state flux (Jss) and permeability coefficient (Kp) were calculated from the permeation profile:

$$\textbf{Jss} = dQ/dt$$

$$\textbf{Kp} = \text{Jss}/C_0$$

where dQ/dt represents the steady-state permeation rate and C_0 represents the initial drug concentration. The enhancement ratio was calculated by comparison with the corresponding control formulation.

2.10 In Vitro Biological Evaluation

The biological activity of free icariin, free curcumin, their combination, and the optimized nano-transfersome-loaded RDMN formulation was evaluated using suitable osteoblast and osteoclast-related in vitro models. Cell viability and proliferation were assessed, followed by evaluation of osteogenic differentiation using alkaline phosphatase (ALP) activity and Alizarin Red S staining. Osteoclast-related activity was assessed using tartrate-resistant acid phosphatase (TRAP) analysis. Expression of representative osteogenic markers, including RUNX2, ALP, COL1A1, and

osteocalcin (BGLAP), and osteoclast-related markers, including NFATc1 and CTSK, was evaluated to investigate the cellular effects of the formulations.

2.11 In Vivo Anti-Osteoporotic Study

The anti-osteoporotic activity was evaluated in female Wistar albino rats weighing 180-220 g. Animals were acclimatized for 7 days under controlled environmental conditions (22 ± 2°C; relative humidity 55 ± 5%; 12-h light/dark cycle) with standard pellet diet and water provided ad libitum. The experimental protocol was conducted following institutional ethical approval and applicable CPCSEA guidelines. Osteoporosis was induced by bilateral ovariectomy, followed by approximately 8 weeks for development of the osteoporotic condition. Animals were divided into seven groups (n = 6/group): normal/sham control, osteoporotic control, alendronate-treated group, icariin-treated group, curcumin-treated group, icariin-curcumin combination group, and optimized nano-transfersome-loaded RDMN patch group.

Alendronate (1 mg/kg, orally, daily), icariin (10 mg/kg, orally, daily), curcumin (50 mg/kg, orally, daily), and the icariin-curcumin combination (10 + 50 mg/kg, orally, daily) were administered according to the experimental design. The optimized nano-transfersome-loaded RDMN patch was applied transdermally at an equivalent optimized dose according to the predetermined treatment schedule. Treatment was continued for 8 weeks. Body weight, general health, and local skin responses were monitored throughout the study. At the end of the treatment period, blood samples and femoral/tibial bones were collected for biochemical, bone-related, and histopathological investigations.

2.12 Biochemical and Bone-Related Evaluation

Serum biochemical parameters, including calcium, phosphorus, alkaline phosphatase (ALP), osteocalcin, and tartrate-resistant acid phosphatase (TRAP), were evaluated. Serum RANKL and osteoprotegerin (OPG) levels were also determined, and the RANKL/OPG ratio was calculated as an indicator of osteoclastogenic activity. Blood samples were allowed to clot for 20-30 min and centrifuged at 3000 rpm for 10 min at 4°C. The separated serum was stored at −20°C until analysis. Calcium, phosphorus, and ALP were estimated using commercial diagnostic kits, whereas osteocalcin, RANKL, and OPG were determined using appropriate ELISA methods. Bone samples were further subjected to bone-density, microarchitectural, and histopathological evaluation according to the experimental protocol.

2.13 Statistical Analysis

Experimental results were expressed as mean ± standard deviation (SD). Statistical analysis was performed using an appropriate statistical software package. Differences among experimental groups were analyzed using suitable statistical tests, with $p < 0.05$ considered statistically significant.

3. RESULTS AND DISCUSSION

3.1 Preformulation and Drug-Excipient Compatibility

Icariin was obtained as a pale-yellow to yellow crystalline powder, while curcumin appeared as a bright-yellow to orange-yellow crystalline powder. Both compounds showed poor aqueous solubility, with curcumin exhibiting particularly limited solubility (0.011 ± 0.002 mg/mL). The solubility of icariin and curcumin in DMSO was substantially higher, at 48.72 ± 1.35 and 32.58 ± 1.12 mg/mL, respectively. The melting points were 231-234°C for icariin and 183-185°C for curcumin. The maximum absorption wavelengths were 270 and 425 nm for icariin and curcumin, respectively. Both compounds showed excellent linearity over 2-12 µg/mL, with R^2 values of 0.9991 and 0.9993, respectively.

Table 1. Selected Preformulation characteristics of icariin and curcumin

Parameter	Icariin	Curcumin
Appearance	Pale yellow/yellow crystalline powder	Bright yellow/orange-yellow crystalline powder
Melting point	231-234°C	183-185°C
Λmax	270 nm	425 nm
Aqueous solubility (mg/mL)	0.38 ± 0.03	0.011 ± 0.002
PBS pH 7.4 (mg/mL)	0.42 ± 0.04	0.012 ± 0.002
DMSO (mg/mL)	48.72 ± 1.35	32.58 ± 1.12

Calibration range	2-12 µg/mL	2-12 µg/mL
Regression equation	y = 0.0718x + 0.0062	y = 0.0746x + 0.0048
R^2	0.9991	0.9993

FTIR analysis showed retention of the characteristic absorption bands of icariin and curcumin in the presence of the selected excipients. No major disappearance, formation of new characteristic bands, or pronounced peak displacement was observed, indicating the absence of evident chemical incompatibility between the phytoconstituents and formulation components.

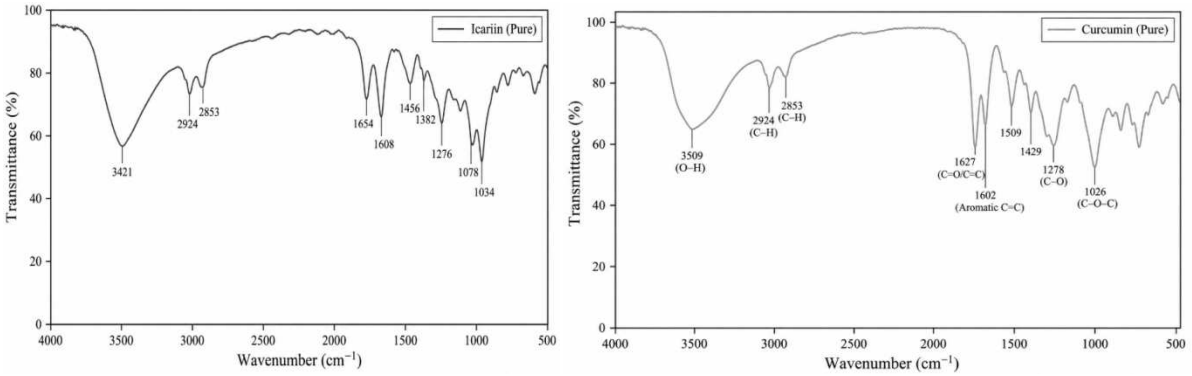


Figure 1. FTIR spectra of icariin, curcumin.

3.2 Development and Optimization of Nano-Transfersomes

Nine nano-transfersome formulations (NT1-NT9) were developed by varying phospholipid and Tween 80 concentrations. All formulations exhibited homogeneous yellow to yellowish-orange appearance without visible phase separation. Vesicle size ranged from 108.6 ± 3.2 to 162.8 ± 5.0 nm, while PDI ranged from 0.158 ± 0.010 to 0.276 ± 0.016. Increasing phospholipid concentration generally increased vesicle size, whereas the presence of Tween 80 influenced vesicle packing and size distribution. NT5, containing 100 mg phospholipid and 20 mg Tween 80, exhibited a vesicle size of 126.4 ± 3.9 nm, the lowest PDI (0.158 ± 0.010), and a zeta potential of −33.6 ± 1.8 mV. The entrapment efficiencies of icariin and curcumin were 93.24 ± 1.08% and 95.18 ± 1.02%, respectively. These characteristics supported the selection of NT5 as the optimized nano-transfersome formulation.

Table 2. Physicochemical characteristics and entrapment efficiency of nano-transfersome formulations

Formulation	Phospholipid (mg)	Tween 80 (mg)	Size (nm)	PDI	Zeta potential (mV)	Icariin EE (%)	Curcumin EE (%)
NT1	50	10	108.6 ± 3.2	0.214 ± 0.015	−23.4 ± 1.4	76.82 ± 1.51	79.46 ± 1.43
NT2	50	20	114.8 ± 3.5	0.198 ± 0.013	−26.1 ± 1.5	81.35 ± 1.38	84.12 ± 1.34
NT3	50	30	120.7 ± 3.8	0.186 ± 0.012	−28.4 ± 1.6	85.64 ± 1.29	87.36 ± 1.26
NT4	100	10	132.5 ± 4.1	0.203 ± 0.014	−30.2 ± 1.7	88.72 ± 1.22	90.18 ± 1.20
NT5	**100**	**20**	**126.4 ± 3.9**	**0.158 ± 0.010**	**−33.6 ± 1.8**	**93.24 ± 1.08**	**95.18 ± 1.02**

NT6	100	30	119.6 ± 3.6	0.171 ± 0.011	−32.4 ± 1.7	91.46 ± 1.14	93.62 ± 1.08
NT7	150	10	162.8 ± 5.0	0.276 ± 0.016	−22.8 ± 1.4	80.46 ± 1.47	84.72 ± 1.39
NT8	150	20	141.3 ± 4.4	0.195 ± 0.013	−29.4 ± 1.6	89.86 ± 1.17	92.14 ± 1.12
NT9	150	30	148.7 ± 4.7	0.218 ± 0.014	−27.1 ± 1.5	90.74 ± 1.13	93.05 ± 1.07

Values are mean ± SD.

The optimized NT5 formulation showed spherical to near-spherical vesicles with well-defined boundaries and no prominent aggregation under TEM. Its deformability index was 18.72 ± 1.16.

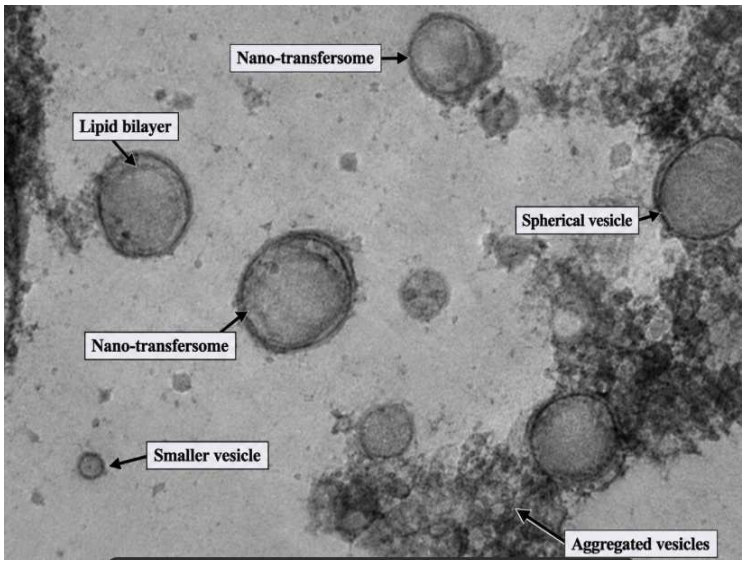


Figure 2. TEM image of optimized NT5 showing spherical/near-spherical nano-transfersomes.

3.3 Development and Optimization of Rapid-Dissolving Microneedles

Five PVA-PVP microneedle formulations were prepared. All formulations exhibited smooth and uniform needle structures without visible cracks or bubbles. Increasing polymer concentration improved mechanical strength and insertion efficiency but also increased dissolution time. MN3 provided a suitable balance between these properties, with a needle height of 710 ± 11 µm, fracture force of 0.36 ± 0.03 N/needle, insertion efficiency of 92.8 ± 2.4%, and dissolution time of 3.1 ± 0.3 min. The formulation also showed high drug content, with 98.4 ± 0.9% icariin and 98.1 ± 0.8% curcumin.

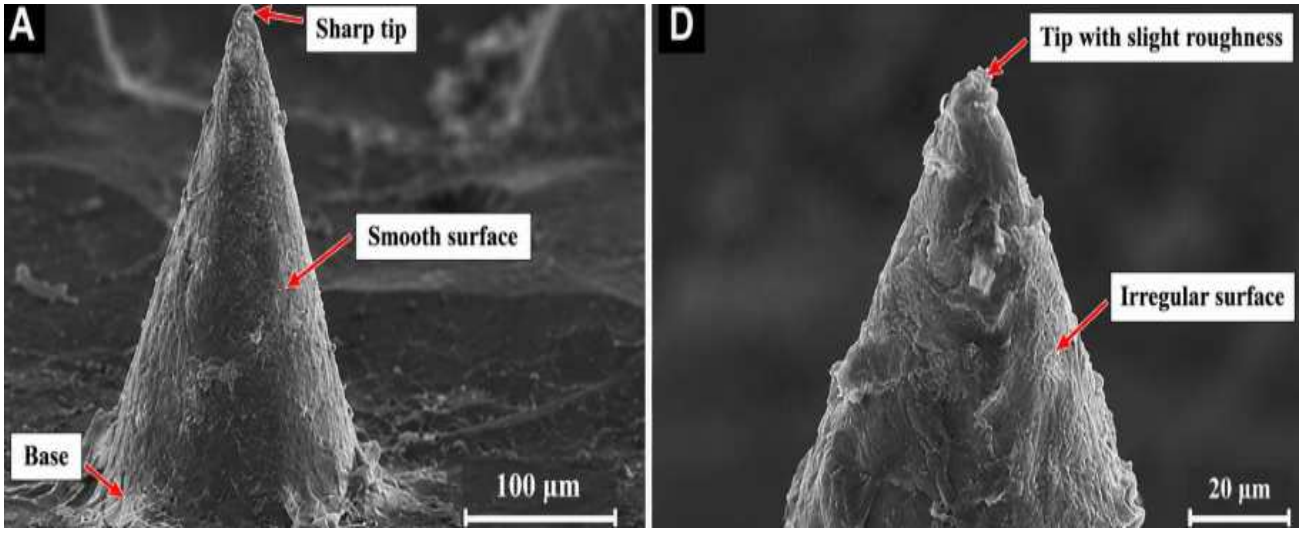


Figure 3. Representative microscopic/SEM image of optimized MN3.

The selection of MN3 was based on the overall balance between mechanical integrity, skin insertion and rapid dissolution rather than maximum performance of any single parameter.

3.4 In-Vitro Drug Release

The optimized MN3 formulation exhibited sustained release of both phytoconstituents over 24 h. Icariin release increased from 15.8 ± 0.8% at 0.5 h to 61.2 ± 1.2% at 3 h and 91.6 ± 0.9% at 12 h, reaching 96.2 ± 0.8% at 24 h. Curcumin release reached 56.4 ± 1.1% at 3 h and 88.7 ± 0.8% at 12 h, with 94.8 ± 0.9% released by 24 h.

Table 4. In-vitro cumulative release of icariin and curcumin from MN3

Time (h)	Icariin (%)	Curcumin (%)
0.5	15.8 ± 0.8	11.9 ± 0.7
1	29.6 ± 1.0	24.8 ± 0.9
2	45.7 ± 1.1	40.6 ± 1.0
3	61.2 ± 1.2	56.4 ± 1.1
6	74.8 ± 1.1	70.2 ± 1.0
8	83.9 ± 1.0	79.8 ± 0.9
12	91.6 ± 0.9	88.7 ± 0.8
24	96.2 ± 0.8	94.8 ± 0.9

Values are mean ± SD.

3.5 In-Vitro Osteoprotective Activity

The biological evaluation demonstrated that the developed delivery systems maintained high cellular viability while increasing osteoblast-associated responses. At 10 µg/mL, cell viability was 94.8 ± 2.4% for free icariin, 93.6 ± 2.6% for free curcumin, 95.7 ± 2.2% for the free combination, 97.4 ± 1.8% for NT5 and 98.1 ± 1.6% for MN3.

Table 5. Selected in-vitro osteoprotective responses

Treatment	Cell viability at 10 µg/mL (%)	Osteoblast proliferation at 72 h (%)	ALP (fold)	Mineralization (%)	TRAP activity (% of control)
Control	100.0	100.0	1.00 ± 0.05	100.0 ± 4.2	100.0 ± 4.5

Free icariin	94.8 ± 2.4	118.6	1.31 ± 0.06	126.8 ± 5.1	78.4 ± 3.9
Free curcumin	93.6 ± 2.6	116.9	1.27 ± 0.05	122.4 ± 4.8	81.2 ± 4.1
Free icariin + curcumin	95.7 ± 2.2	128.4	1.52 ± 0.07	148.6 ± 5.7	66.7 ± 3.6
NT5	97.4 ± 1.8	142.7	1.86 ± 0.08	181.9 ± 6.3	49.8 ± 3.1
MN3	98.1 ± 1.6	151.8	2.14 ± 0.09	216.7 ± 7.1	38.6 ± 2.8

Values are mean ± SD where reported.

Osteoblast proliferation increased progressively with treatment duration. At 72 h, the free icariin-curcumin combination increased proliferation to 128.4%, compared with 142.7% for NT5 and 151.8% for MN3. Similarly, ALP activity increased from 1.52 ± 0.07-folds with the free combination to 1.86 ± 0.08-folds with NT5 and 2.14 ± 0.09-fold with MN3. Alizarin Red S staining showed enhanced extracellular matrix mineralization, increasing from 148.6 ± 5.7% with the free combination to 181.9 ± 6.3% with NT5 and 216.7 ± 7.1% with MN3. In parallel, TRAP activity decreased to 66.7 ± 3.6%, 49.8 ± 3.1% and 38.6 ± 2.8% of control with the free combination, NT5 and MN3, respectively. The combined increase in osteoblast proliferation, ALP activity and mineralization together with reduced TRAP activity indicates that the developed system influenced both osteogenic and osteoclast-associated responses.

3.6 Molecular Marker Analysis

The molecular findings supported the functional cellular results. The free icariin-curcumin combination increased RUNX2, ALP, COL1A1 and BGLAP expression compared with the untreated control, while NT5 produced a further increase. MN3 showed the highest relative expression of these osteogenic markers. Conversely, NFATc1 and CTSK expression decreased following treatment, with the greatest reduction observed with MN3.

Table 6. Relative expression of osteogenic and osteoclast-related markers

Treatment	RUNX2	ALP	COL1A1	BGLAP	NFATc1	CTSK
Control	1.00 ± 0.06	1.00 ± 0.05	1.00 ± 0.06	1.00 ± 0.05	1.00 ± 0.06	1.00 ± 0.05
Free icariin + curcumin	1.62 ± 0.09	1.57 ± 0.08	1.51 ± 0.09	1.55 ± 0.08	0.67 ± 0.05	0.63 ± 0.04
NT5	1.98 ± 0.11	1.91 ± 0.10	1.87 ± 0.10	1.92 ± 0.11	0.48 ± 0.04	0.45 ± 0.04
MN3	2.34 ± 0.12	2.28 ± 0.11	2.21 ± 0.12	2.26 ± 0.12	0.36 ± 0.03	0.33 ± 0.03

Values are relative fold expression ± SD (n = 3); untreated control = 1.0.

3.7 In-Vivo Anti-Osteoporotic Activity

No mortality or major treatment-related toxicity was observed during the experimental period. The osteoporotic control animals showed reduced activity and grooming compared with the normal control, whereas treated animals maintained satisfactory general health. The osteoporotic control showed marked alterations in serum biochemical parameters. Calcium and phosphorus decreased to 8.41 ± 0.29 and 4.36 ± 0.19 mg/dL, respectively, while ALP and TRAP increased to 136.8 ± 6.2 and 5.86 ± 0.27 U/L. Osteocalcin decreased to 11.2 ± 0.9 ng/mL. Treatment with the free icariin-curcumin combination partially corrected these changes, whereas NT5 produced greater improvement. MN3 produced calcium and phosphorus concentrations of 10.01 ± 0.30 and 5.56 ± 0.23 mg/dL, respectively, with ALP, TRAP and osteocalcin values of 88.9 ± 4.6 U/L, 3.51 ± 0.19 U/L and 18.0 ± 1.3 ng/mL, respectively.

Table 7. Serum biochemical and osteoclast-regulatory parameters

Group	Ca (mg/dL)	P (mg/dL)	ALP (U/L)	Osteocalcin (ng/mL)	TRAP (U/L)	RANKL (pg/mL)	OPG (pg/mL)	RANKL/OPG
Normal control	10.24 ± 0.32	5.82 ± 0.21	82.6 ± 4.8	18.4 ± 1.2	3.42 ± 0.18	42.8 ± 2.6	58.6 ± 3.1	0.73 ± 0.05

Osteoporotic control	8.41 ± 0.29	4.36 ± 0.19	136.8 ± 6.2	11.2 ± 0.9	5.86 ± 0.27	78.6 ± 4.1	40.9 ± 2.7	1.92 ± 0.12
Standard treatment	9.72 ± 0.31	5.34 ± 0.20	94.3 ± 5.1	16.7 ± 1.1	3.91 ± 0.21	48.9 ± 2.9	58.2 ± 3.2	0.84 ± 0.06
Free icariin + curcumin	9.28 ± 0.30	4.91 ± 0.22	108.6 ± 5.7	14.8 ± 1.0	4.47 ± 0.23	60.7 ± 3.3	44.3 ± 2.8	1.37 ± 0.09
NT5	9.71 ± 0.28	5.28 ± 0.21	96.7 ± 4.9	17.1 ± 1.2	3.78 ± 0.20	50.8 ± 2.8	59.1 ± 3.3	0.86 ± 0.06
MN3	10.01 ± 0.30	5.56 ± 0.23	88.9 ± 4.6	18.0 ± 1.3	3.51 ± 0.19	45.6 ± 2.7	66.1 ± 3.5	0.69 ± 0.05

Values are mean ± SD (n = 6).

The RANKL/OPG ratio increased from 0.73 ± 0.05 in normal controls to 1.92 ± 0.12 in osteoporotic controls. Treatment reduced the ratio to 1.37 ± 0.09 with the free combination, 0.86 ± 0.06 with NT5 and 0.69 ± 0.05 with MN3. The associated reduction in RANKL and increase in OPG suggest restoration of the osteoclast-regulatory balance.

3.8 Bone Mineral Density, Bone Morphometry and Microarchitecture

Osteoporosis induction resulted in a substantial reduction in BMD from 0.214 ± 0.009 g/cm² in the normal control to 0.151 ± 0.008 g/cm² in the osteoporotic control. BMD increased to 0.181 ± 0.007 g/cm² with the free icariin-curcumin combination, 0.194 ± 0.008 g/cm² with NT5 and 0.207 ± 0.009 g/cm² with MN3. BMC followed a similar pattern, decreasing from 0.482 ± 0.021 g in the normal control to 0.346 ± 0.019 g in the osteoporotic control and increasing to 0.468 ± 0.020 g following MN3 treatment.

Table 8. Bone mineral density, bone mineral content and selected structural parameters

Group	BMD (g/cm²)	BMC (g)	Cortical thickness (µm)	Trabecular thickness (µm)	Trabecular number (mm⁻¹)
Normal control	0.214 ± 0.009	0.482 ± 0.021	412 ± 18	126 ± 7	3.82 ± 0.18
Osteoporotic control	0.151 ± 0.008	0.346 ± 0.019	318 ± 16	91 ± 6	2.74 ± 0.15
Standard treatment	0.198 ± 0.008	0.452 ± 0.020	391 ± 17	117 ± 6	3.54 ± 0.17
Free icariin + curcumin	0.181 ± 0.007	0.411 ± 0.018	362 ± 16	105 ± 6	3.21 ± 0.16
NT5	0.194 ± 0.008	0.443 ± 0.019	384 ± 17	114 ± 6	3.47 ± 0.17
MN3	0.207 ± 0.009	0.468 ± 0.020	402 ± 18	122 ± 7	3.71 ± 0.18

Values are mean ± SD (n = 6).

The osteoporotic control also exhibited deterioration of bone microarchitecture, with BV/TV, trabecular thickness and trabecular number decreasing and trabecular separation and SMI increasing. Treatment with NT5 and particularly MN3 improved these parameters.

Table 9. Bone microarchitectural parameters

Group	BV/TV (%)	Tb.Th (µm)	Tb.N (mm⁻¹)	Tb.Sp (µm)	SMI
Normal control	28.6 ± 1.4	126 ± 7	3.82 ± 0.18	184 ± 9	1.18 ± 0.08
Osteoporotic control	17.4 ± 1.2	91 ± 6	2.74 ± 0.15	268 ± 12	2.01 ± 0.11
Standard treatment	26.1 ± 1.3	117 ± 6	3.54 ± 0.17	201 ± 10	1.32 ± 0.09

Free icariin + curcumin	22.8 ± 1.3	105 ± 6	3.21 ± 0.16	229 ± 11	1.58 ± 0.10
NT5	25.4 ± 1.3	114 ± 6	3.47 ± 0.17	207 ± 10	1.37 ± 0.09
MN3	27.8 ± 1.4	122 ± 7	3.71 ± 0.18	191 ± 9	1.23 ± 0.08

Values are mean ± SD (n = 6).

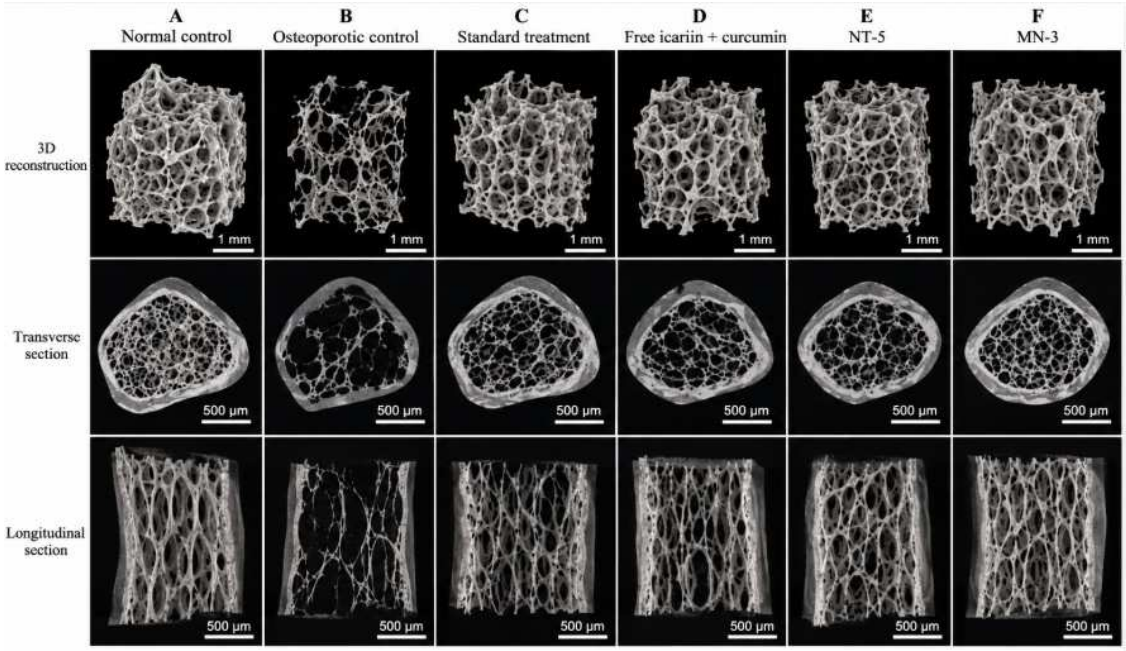


Figure 4 : Representative micro-CT images of bone microarchitecture in experimental groups.

The improvement in BMD, BMC and structural parameters was consistent with the biochemical findings. The MN3 group showed restoration of bone characteristics toward the normal-control profile, including increased trabecular thickness and number and reduced trabecular separation and SMI.

3.9 Overall Discussion

The findings demonstrate the successful development of an icariin-curcumin nano-transfersome-loaded rapid-dissolving microneedle system. The initial preformulation study established the poor aqueous solubility of the two phytoconstituents, supporting the selection of a lipid-based nanocarrier. Among the nine nano-transfersome formulations, NT5 provided a favorable combination of vesicle size, PDI, surface charge and entrapment efficiency and was therefore selected for incorporation into the microneedle matrix. The subsequent microneedle optimization demonstrated the importance of balancing polymer concentration with mechanical strength, insertion ability and dissolution behavior. MN3 provided an appropriate combination of these properties and showed high drug content. The release profile further demonstrated efficient liberation of both phytoconstituents over 24 h.

The in-vitro biological results indicated that the combination of icariin and curcumin produced greater osteoblast-associated responses than either phytoconstituent alone. Importantly, incorporation into NT5 and subsequently MN3 was associated with further increases in osteoblast proliferation, ALP activity and mineralization, together with reductions in TRAP activity. Molecular analysis supported these findings by demonstrating increased expression of osteogenic markers and reduced expression of osteoclast-related markers. The in-vivo findings extended these observations to the experimental osteoporosis model. Osteoporotic animals demonstrated alterations in mineral homeostasis, bone turnover and the RANKL/OPG regulatory system, together with reduced BMD, BMC and deteriorated bone microarchitecture. Treatment with the free icariin-curcumin combination, NT5 and MN3 progressively improved these parameters. The MN3 formulation produced changes toward the normal-control profile across biochemical, molecularly related and structural bone endpoints.

Taken together, the results indicate that the nano-transfersome-loaded rapid-dissolving microneedle platform improved the overall delivery performance of the icariin-curcumin combination and produced consistent osteogenic

and anti-osteoclast-associated responses in the investigated in-vitro and in-vivo models. The findings provide a formulation-development basis for further investigation of this delivery approach for osteoporosis.

4. CONCLUSION

The present study successfully developed and evaluated an icariin-curcumin co-loaded nano-transfersome-based rapid-dissolving microneedle patch for potential application in osteoporosis management. Among the developed nano-transfersome formulations, NT5 containing 100 mg phospholipid and 20 mg Tween 80 demonstrated a favorable combination of vesicle size, PDI, zeta potential, and high entrapment efficiencies for both icariin and curcumin. Incorporation of the optimized nano-transfersomes into a PVA-PVP microneedle matrix resulted in the selection of MN3, which exhibited satisfactory mechanical strength, efficient skin insertion, rapid dissolution, and high drug content.

The optimized MN3 formulation provided sustained release of both phytoconstituents over 24 h and demonstrated enhanced osteoblast-associated activity, including increased cellular proliferation, ALP activity and matrix mineralization, together with reduced TRAP activity. The molecular findings further supported these effects through increased expression of osteogenic markers and reduced expression of osteoclast-related markers. In the ovariectomized osteoporosis model, MN3 treatment improved serum calcium, phosphorus, osteocalcin, ALP, TRAP, RANKL and OPG profiles and produced favorable changes in BMD, BMC, bone morphometry and trabecular microarchitecture.

Overall, the findings demonstrate that combining nano-transfersomal delivery with a rapid-dissolving microneedle platform can provide a promising strategy for the delivery of icariin and curcumin and for addressing both osteogenic and osteoclast-associated aspects of experimental osteoporosis. The optimized formulation warrants further investigation, particularly through comprehensive skin-permeation studies, long-term stability assessment, and additional pharmacokinetic and translational studies, before potential clinical application.

Acknowledgement

The authors would like to express their sincere gratitude to all individuals and institutions whose support and encouragement contributed to the completion of this review article.

Conflict of Interest

The authors declare that there is no conflict of interest associated with the publication of this article.

5. References

- Benson, H. A. E. (2006). Transfersomes for transdermal drug delivery. *Expert Opinion on Drug Delivery, 3*(6), 727-737.
- Cevc, G., & Blume, G. (1992). Lipid vesicles penetrate into intact skin owing to the transdermal osmotic gradients and hydration force. *Biochimica et Biophysica Acta, 1104*(1), 226-232.
- Compston, J. E., McClung, M. R., & Leslie, W. D. (2019). Osteoporosis. *The Lancet, 393*(10169), 364-376.
- Firoz, M., & Parmar, S. (2026). Design and characterization of lurasidone-loaded niosomes for improved oral bioavailability and targeted brain delivery. *Global Journal of Pharmaceutical and Scientific Research, 2*(6), 944-965. https://doi.org/10.66204/GJPSR-944-2026-2-6-6
- Fu, B., Yu, S., Chen, S., & Hu, B. (2025). Icariin against osteoporosis: A review of advances in molecular mechanisms to biomedical applications. *Frontiers in Pharmacology, 16*, 1688847. https://doi.org/10.3389/fphar.2025.1688847
- Hewlings, S. J., & Kalman, D. S. (2017). Curcumin: A review of its effects on human health. *Foods, 6*(10), 92.
- Ita, K. (2017). Dissolving microneedles for transdermal drug delivery: Advances and challenges. *Biomedical Pharmacotherapy, 93*, 1116-1127.
- Kumar, S., Maurya, V. K., & Kumar, K. (2026). Ethosomal gel for enhanced topical delivery: A review. *Global Journal of Pharmaceutical and Scientific Research, 2*(8), 1217-1239. https://doi.org/10.66204/GJPSR-1217-2026-2-8-3
- Moawad, F., Pouliot, R., & Brambilla, D. (2025). Dissolving microneedles in transdermal drug delivery: A critical analysis of limitations and translation challenges. *Journal of Controlled Release, 383*, 113794. https://doi.org/10.1016/j.jconrel.2025.113794
- Nelson, K. M., Dahlin, J. L., Bisson, J., Graham, J., Pauli, G. F., & Walters, M. A. (2017). The essential medicinal chemistry of curcumin. *Journal of Medicinal Chemistry, 60*(5), 1620-1637.

- Pal, A., Maurya, V. K., & Kumar, K. (2026). Liposomes as drug delivery systems: A comprehensive review with recent advances. *Global Journal of Pharmaceutical and Scientific Research, 2*(7), 1124-1144. https://doi.org/10.66204/GJPSR-1124-2026-2-7-6
- Prausnitz, M. R., & Langer, R. (2008). Transdermal drug delivery. *Nature Biotechnology, 26*(11), 1261-1268.
- Wang, Z., Wang, D., Yang, D., Zhen, W., Zhang, J., & Peng, S. (2018). The effect of icariin on bone metabolism and its potential clinical application. *Osteoporosis International, 29*(3), 535-544.
- Wasiullah, M., Yadav, P., Musharraf, M., & Yadav, M. K. (2025). Systematic review on nanotechnology for phytomedicine research and drug development. *Global Journal of Pharmaceutical and Scientific Research, 1*(5).
- Yadav, V. (2026). Comprehensive study of turmeric and its main compound curcumin. *Global Journal of Pharmaceutical and Scientific Research, 2*(8), 1317-1326. https://doi.org/10.66204/GJPSR-1317-2026-2-8-8
- Yang, S. L., Wang, J. X., Ma, F. E., He, J. H., Zhang, A., Sun, X. M., Wei, Y., & Wang, Y. (2025). Comprehensive systematic review and meta-analysis on the therapeutic efficacy of curcumin in osteoporosis: Unveiling mechanisms and preclinical evidence. *Frontiers in Nutrition, 12*, 1590256. https://doi.org/10.3389/fnut.2025.1590256
- Zhao, W., Li, X., Gu, H., Xu, J., & Bi, H. (2025). Icariin regulates the Hippo/TAZ signaling pathway to promote osteogenic differentiation and bone remodeling in osteoporosi. *Biochemical and Biophysical Research Communications, 792*, 152888.
- Zhuo, Y., Wang, F., Lv, Q., & Fang, C. (2025). Dissolving microneedles: Drug delivery and disease treatment. *Colloids and Surfaces B: Biointerfaces, 250*, 114571. https://doi.org/10.1016/j.colsurfb.2025.114571.